

Two rapid oscillations in the magnetoresistance in the field-induced spin-density-wave state of $(\text{TMTSF})_2\text{ClO}_4$

Ok-Hee Chung

Department of Physics, Sunchon University, Sunchon 540 742, South Korea

W. Kang

Department of Physics, Ewha Womans University, Seoul 120 750, South Korea

D. L. Kim and C. H. Choi

Korea Basic Science Institute, Taejon 305 333, South Korea

(Received 31 August 1999)

We report a systematic study of longitudinal and transverse magnetoresistance in the quasi-one-dimensional organic conductor $(\text{TMTSF})_2\text{ClO}_4$. We found two distinctly different quantum (rapid) oscillations (RO's) at different temperature regions in the field-induced spin-density-wave (FISDW) phase. For temperature sweeps in a fixed field, a resistance peak is observed at T^* which depends on the field. Surprisingly, the type of RO is correlated with $T^*(H)$. The difference between two oscillations leads us to establish subphases in the main FISDW phase of $(\text{TMTSF})_2\text{ClO}_4$. We also found the low-field boundary of McKernan's 3.5 K phase from a sudden increase of resistance. Our results conclude that the separate SDW transition on each pair of the Fermi surfaces is possibly responsible for subphases in the FISDW phase.

I. INTRODUCTION

The $(\text{TMTSF})_2X$ family of quasi-one-dimensional (Q1D) conductors exhibit many interesting phenomena such as superconductivity, anion ordering (AO), spin-density wave (SDW), a cascade of field-induced SDW (FISDW), quantized Hall effect, angular oscillations in magnetoresistance and in magnetization, and rapid oscillations (RO's).¹ Most of these phenomena result from the highly anisotropic Fermi surface (FS) which consists of only open sheets. The low dimensionality allows a rich phase diagram as pressure, magnetic field, temperature, and anion ordering change.

At low temperature, the magnetic field along the c^* , the least conducting direction, leads to a cascade of FISDW transitions, which are characterized by the quantized Hall plateaus. The cascade of FISDW transitions are understood in terms of the field-dependent nesting wave vector ($Q_x = 2k_F + nebH/hc$), which adjusts itself to maintain the Fermi level in the largest energy gap, where n is the quantum Hall index.² For the ClO_4 , there is an extremely stable quantum Hall-semimetallic phase which persists from 8 to 28 T at 0.5 K. The high-field state (HFS) above 28 T had been known as the reentrant metallic phase. However, recent extensive studies of transport and magnetization indicated that the HFS is not a reentrant metallic state. A phase diagram was proposed with an additional SDW phase above 28 T.³

A type of quantum oscillations or RO's, reminiscent of Shubnikov-de Haas (SdH) oscillations, has been seen in the magnetoresistance for most of the TMTSF compounds. The RO having a periodicity in the inverse field has a unique temperature dependence. The amplitude has a maximum at ~ 3 K and vanishes at low temperatures.⁴⁻¹³ The oscillation periods are 200–300 T. The oscillations have been observed

both in the SDW and in the metallic (M) phases for the ClO_4 salt, but detected only in the SDW phase for PF_6 and AsF_6 salts. Nonetheless, corresponding oscillations in the magnetization [the de Haas-van Alphen effect (dHvA)] have been detected only in the ClO_4 salt and only in the FISDW phase. Since the zero-field FS is open, their origin must differ from that of the standard quantum oscillations of two-dimensional metals. Recently, a number of theories have been proposed for the RO, but none of them has been entirely consistent with all the experimental results.¹⁴⁻¹⁸

In order to explain the difference between PF_6 and ClO_4 salts, attention has been paid to the anion ordering transition in ClO_4 . In the slowly cooled ClO_4 salt, anion ordering (AO) takes place at ~ 24 K, and causes a superlattice potential with a wave vector $\mathbf{Q} = (0, \pi/b, 0)$. The potential opens a gap on the original FS and two pairs of open Fermi sheets are formed as sketched in Fig. 1(a). Since the open sheets of FS at the same side are very close to each other, the Stark quantum interference can easily happen at zone boundaries ($k_y = \pm \pi/2b$) between the two sheets where electrons proceed along the same direction as shown in Fig. 1(b). The oscillations observed in the resistance are attributed to the Stark quantum interference oscillation characterized by a simple sinusoidal waveform with the periodicity $\hbar cA/H$ where A is the k -space area of the loop.¹⁹ This explains why the RO in the resistance exists in the M phase of the ClO_4 .^{7,12} The interference effect is not expected for the PF_6 salt without anion ordering, which is consistent with experimental results.

On the other hand, Brooks *et al.*²⁰ proposed that the RO in the HFS above 28 T results from the magnetic breakdown (MB) of the reconstructed, nested FS topology. The temperature and field dependence of the RO is explained with the competition between MB and Bragg reflection (BR) prob-

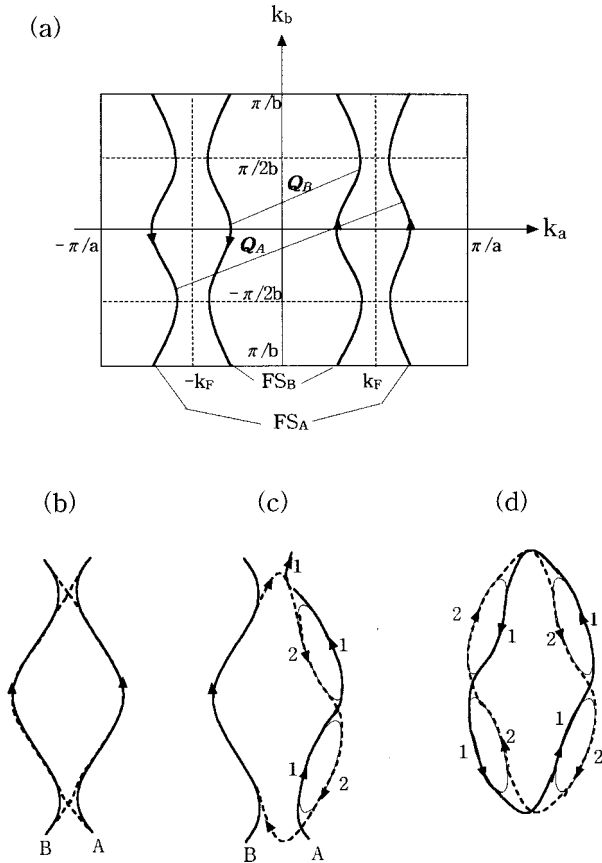


FIG. 1. Schematic diagram of the FS in $(\text{TMTSF})_2\text{ClO}_4$ in the presence of the AO. \mathbf{Q}_A and \mathbf{Q}_B correspond to the SDW nesting vectors for the FS_A and FS_B , respectively. (b) The Stark interference oscillation between two parallel electron motions in the M phase. (c) The SDW nested FS_A with magnetic breakdown (MB) and Bragg reflection (BR) and the metallic (M) FS_B can lead to either the SdH oscillation in the closed orbit by the path 2 or the Stark oscillation by the path 1 at $T^* < T < 5.5$ K. (d) At $T < T^*$, the reconstructed FS can lead to the SdH oscillation after the second SDW transition occurs on the FS_B .

abilities, along with Lifshitz-Kosevich reduction factors. According to the authors, the FS sheets in the HFS are expected to be perfectly nested with each other. In this sense, the electronic state in the HFS for the ClO_4 salt may be similar to that in the SDW phase for the PF_6 salt.

Although extensive studies have been made to understand the mechanism of the RO for the TMTSF system so far, the mechanism of the RO in the main FIDSW phase between 8 and 28 T for the ClO_4 salt is still in question. In order to understand it in relation to the FIDSW phase, we systematically investigate temperature and field dependences of the longitudinal ($H \parallel c^* I \parallel c^*$) and transverse ($H \parallel c^*, I \parallel a$) magnetoresistances between 8 and 20 T in the temperature range of 0.05 to 20 K. We report discoveries such as two different types of RO's, anomalous temperature and field dependences of their amplitudes, and the correlation between resistances and the RO's. We discuss the two distinct RO's in the main FIDSW phase in relation to the separate SDW transitions between two pairs of FS due to the AO. Our results conclude that new subphases may exist inside the main FIDSW phase of the ClO_4 salt.

II. EXPERIMENTS

The experiments reported here were carried out at the Korea Basic Science Institute in Taejeon, Korea. Single crystals of the ClO_4 salt were synthesized electrochemically. The typical size of the crystals is $\sim 3 \times 0.6 \times 0.1 \text{ mm}^3$. Three samples were studied in a 10 mK dilution refrigerator with a 20 T superconducting magnet. The samples were aligned with the c^* axis along the magnetic field. The voltage and the current were applied either along the highly conducting a axis or along the least conducting c^* axis for the sample. We denote that the R_{xx} (R_{zz}) is the voltage along the $a(c^*)$ axis divided by the current along the $a(c^*)$ axis. The applied current was typically a $100 \mu\text{A}$. Six gold wires ($\phi = 15 \mu\text{m}$) were attached to the sample using silver paste.

For the experiments, the samples were cooled more slowly than 6 mK/min through the AO transition (from 34 to 16 K) to achieve a very well relaxed state. Temperature was monitored and controlled using a RuO_2 thermometer and a cernox sensor mounted within 5 mm from the samples.

III. RESULTS

A. Two types of rapid oscillations

Figures 2(a) and 2(b) show a magnetic-field dependence of the R_{zz} and the R_{xx} at constant temperatures. The SdH-like oscillations are clearly seen at all low temperatures, superposed on the background with the FIDSW transitions for both magnetoresistances. The transition field of the main FIDSW phase, increases with increasing temperature as shown in both of the R_{zz} and R_{xx} , in agreement with the previous reports.

For low temperatures below 0.5 K, a sharp peak develops between 6 and 8 T in the R_{xx} but much less in the R_{zz} . It shifts toward higher field and becomes broader as temperature increases, and then disappears completely above 1.5 K. Interestingly, this anomalous peak of the R_{xx} corresponds to the negative Hall resistance state as shown in the inset of Fig. 2(a). The peak feature in the R_{xx} for the negative Hall state was also observed in PF_6 (Refs. 3,22) and ClO_4 . For the present, the fact that the longitudinal magnetoresistance (R_{xx}) is much larger when the system is in the negative quantized Hall state is not understood.

As shown in Fig. 2, field dependences of the R_{zz} and the R_{xx} vary with temperature even in the same main FIDSW phase. We note that the background resistance grows with increasing temperature until ~ 1.5 K for the R_{zz} (~ 2.0 K for the R_{xx}) then decreases above this temperature. This fact indicates that the resistance would have a maximum around these temperatures in the temperature sweep. In fact, we observed a peak in temperature dependence of the R_{zz} and the R_{xx} as shown in Fig. 5.

In the R_{zz} , oscillations appear as the sample enters in the FIDSW phase and its amplitude grows gradually as the magnetic field increases. The amplitude seems to grow with increasing temperature until 1.0 K. At 1.2 K, however, the oscillation is suddenly corrupted. Then, in temperature higher than 1.5 K, new oscillations emerge. As the temperature increases further beyond 5.5 K, the system enters in the

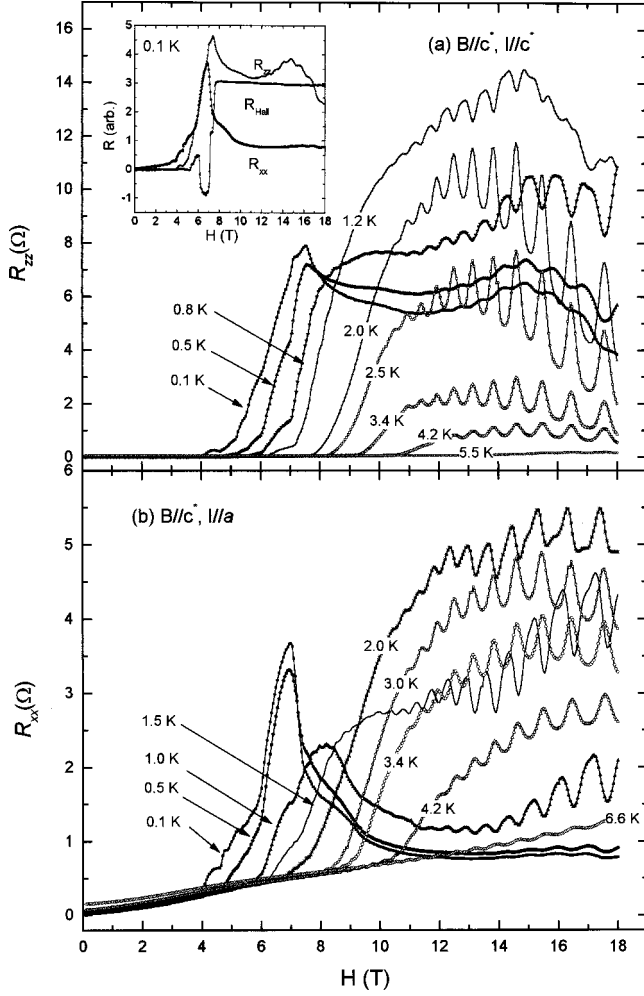


FIG. 2. Magnetoresistance and quantum oscillation behavior of $(\text{TMTSF})_2\text{ClO}_4$ in field sweeps at various temperatures (a) Resistance along the c^* axis, R_{zz} . Inset: Comparison of the Hall resistance, R_{xx} and R_{zz} at 0.1 K. (b) Resistance along the a axis, R_{xx} .

M phase and the oscillations are not observable anymore. In the R_{xx} , the oscillation features below 1.5 K are also different from those above 2.0 K. By the way, the RO is observable even in the M phase above 5.5 K unlikely in the R_{zz} .

To see the RO more clearly, we plotted the $\text{RO}_z \equiv \delta R_{zz}/R_{0z} = (R_{zz} - R_{0z})/R_{0z}$ and $\text{RO}_x \equiv \delta R_{xx}/R_{0x} = (R_{xx} - R_{0x})/R_{0x}$ at various temperatures in Figs. 3(a) and 3(b). Here, the $R_{0z(0x)}$ denotes the nonoscillatory background resistance of the $R_{zz(xx)}$. As shown in the figures, the RO's are periodic in the inverse field with the fundamental frequency F of 260 T. The second harmonic with the frequency $2F$ is observed in addition to the fundamental oscillation in both resistances.

In the main FISDW phase, the RO exhibits some interesting features. At temperatures higher than 1.5 K for the RO_z (3.0 K for the RO_x), the oscillations have *minima* for $260/H = 15, 16, 17, \dots$. However, the oscillations below 1.0 K have *maxima* (not minima) at the same field. We found that the various wave shapes in Fig. 3 can be easily simulated by combinations of the primary and the second harmonics. Below 1.2 K, we suppose that the wave has the form

$$Y_B(H) = C \cos(260/H) + D \cos(2 \times 260/H), \quad (3.1)$$

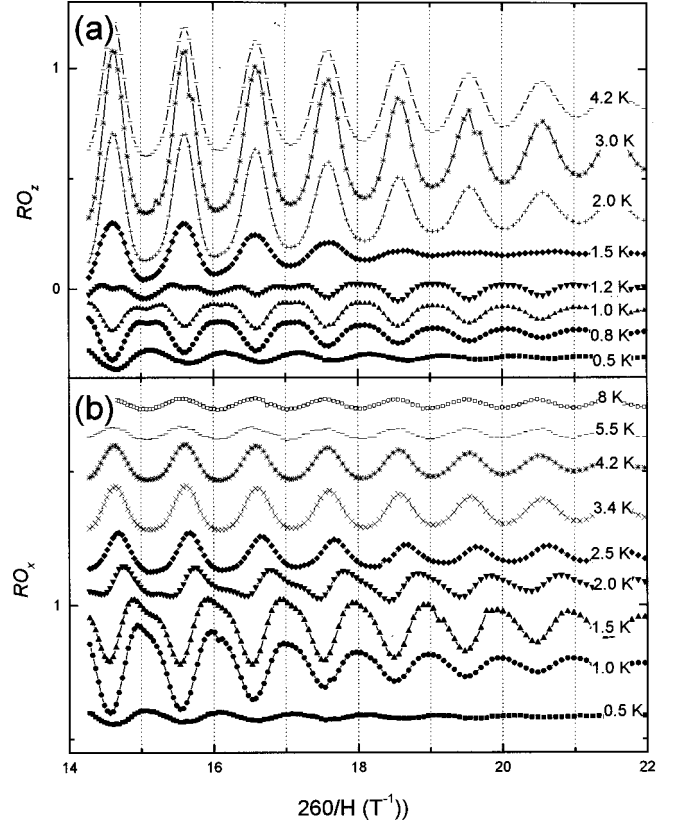


FIG. 3. (a) $\text{RO}_z \equiv \delta R_{zz}/R_{0z} = (R_{zz} - R_{0z})/R_{0z}$ and (b) $\text{RO}_x \equiv \delta R_{xx}/R_{0x} = (R_{xx} - R_{0x})/R_{0x}$ curves at various temperatures.

where C and D represent field- and temperature-dependent amplitudes of the primary and the second harmonics, respectively. On the other hand, above 1.5 K, the oscillation wave form becomes

$$Y_A(H) = C' \cos(260/H + \pi) + D' \cos(2 \times 260/H + \pi), \quad (3.2)$$

whose phase is different by π from $Y_B(H)$. With an adequate combination of arbitrary C and D (C' and D'), we are able to obtain all the waveforms of Fig. 3.

The RO_z at 1.2 K results from the coexistence of the two oscillations reflecting the phase change of RO's across this temperature. In addition, the peaks of the oscillations above 1.5 K are narrower, while the oscillations are more harmonic below 1.2 K. These show that the shape, amplitude, and phase of the oscillations change completely as the temperature crosses 1.2 K. From the above facts, we conclude that the two distinct RO's in the resistance are present at different temperature regions in the FISDW phase above 8 T. Hereafter, we denote the RO which are evident at higher and lower temperatures as ‘‘ RO_A ’’ and ‘‘ RO_B ,’’ respectively. Since the shape, amplitude, and phase between the two RO's are distinct, their mechanisms would be different. Comparing the RO_x with the RO_z , the crossover between two RO's takes place broadly and at higher temperature in the RO_x than in the RO_z as shown in Fig. 3(b). It is also interesting that the type of RO changes even inside of the same FISDW phase. However, the phase and frequency of RO in the R_{xx} remain the same through the transition to the M phase [see Fig. 3(b)].

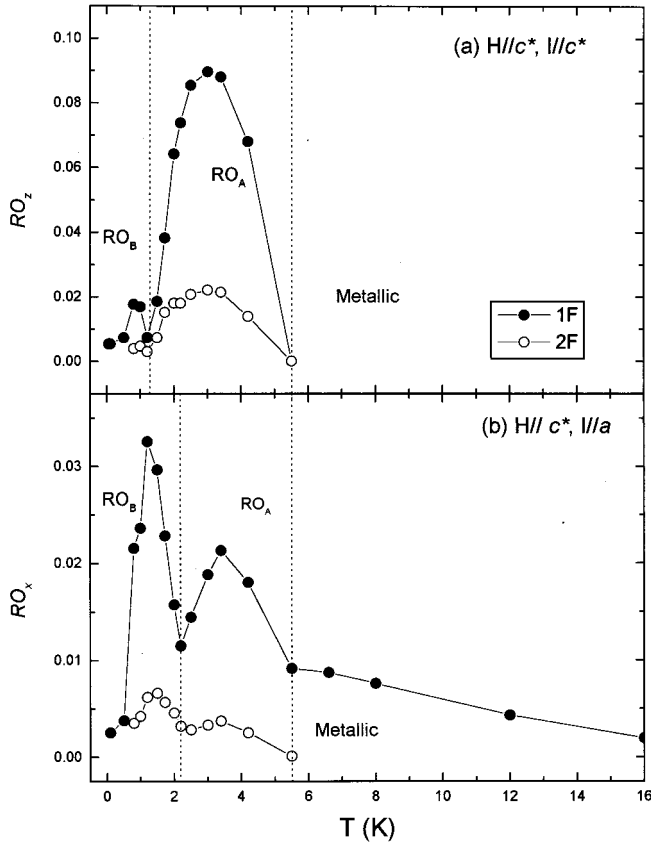


FIG. 4. Temperature dependence of the FT amplitude of (a) RO_z (b) RO_x . Open and solid symbols correspond to the amplitudes of the primary and the second harmonics, respectively. Dotted lines indicate phase separations of the RO_A , RO_B , and M phases.

B. The amplitude of the rapid oscillations

Temperature dependences of Fourier transformed (FT) amplitudes of RO_z and RO_x are plotted in Figs. 4(a) and 4(b). The solid and open symbols indicate the fundamental and the second harmonics, respectively. The RO's in the FISDW phase below 5.5 K consist of the fundamental and the second harmonics. Above 5.5 K, the RO_z disappears and the RO_x consists of only the fundamental one. The amplitude of the fundamental harmonic of the RO_x changes discontinuously at 5.5 K, where the transition to the M phase takes place. The FT amplitude in the M phase is smaller than that in the FISDW phase and decreases with increasing temperature as shown in Fig. 4(b). The absence of the RO_z and of the second harmonic of the RO_x confirm that the RO in the M phase is due to the Stark quantum interference effect. However, unlike the typical Stark oscillations,¹⁹ the oscillations in our data are strongly temperature dependent. The temperature dependence of the amplitude can be explained if we assume that the scattering time τ in the Stark effect is equal to that deduced from the resistance ($\rho = m/ne^2\tau$) which increases with increasing temperature.

The amplitudes of the fundamental and the second harmonics show two anomalous peaks at ~ 1.0 K and ~ 3.0 K in the RO_z (~ 1.2 and ~ 3.4 K in the RO_x), respectively. Above 1.5 K, the observed oscillations are mainly due to RO_A , and below 1.2 K are due to RO_B . The amplitude minimum at ~ 1.5 K in the RO_z (~ 2.0 K in the RO_x) indicates

the boundary between RO_B and RO_A . The amplitude of the RO_A above ~ 1.2 K in the RO_z (~ 2.1 K in the RO_x) has a maximum at ~ 3 K. The amplitude of RO_B below ~ 1.2 K also has a maximum at ~ 1.0 K. This is in contradiction to Uji *et al.*'s report,¹² where there was no evidence of two distinct RO's in the a -axis resistance and the amplitude of the RO had a maximum at ~ 2 K.

In magnetization measurement, McKernan *et al.*³ pointed out that the phase of the RO at 2 K is reversed from that at 4.5 K. Later, Uji *et al.*²¹ found two distinctly different RO's (RO I and RO II) in ClO_4 salt in the magnetization above 20 T and below 6 K. Both exhibit the same frequency but different phase by π . According to their report, the RO I is dominant above the 3.5 K and its amplitude has a maximum at ~ 4 K. The RO II at low temperatures below ~ 3 K increases monotonically with decreasing temperature. The oscillation "RO I" ("RO II") might correspond to RO_A (RO_B) in our results. However, in our resistance measurements, the two types of RO's exist in the fields lower than 20 T and both of them have maxima at ~ 1.0 K and at ~ 3 K in the RO_z . The fact that both RO_A and RO_B have maxima is not analogous with the RO's in the magnetization. The discrepancy between the two measurements comes from the fact that the lowest temperature in the magnetization measurement (See Figs. 2 and 3 in Ref. 21) is 0.9 K, which turns out to be the RO_B maximum in our data. In addition, our observation of two RO's in far lower fields than in the magnetization may be due to better quality and well relaxed samples.

C. Temperature dependence of the resistance

Figures 5(a) and 5(b) present the temperature dependence of the R_{xx} and R_{zz} in constant fields. Both have a maximum at T^* . Above T^* , the resistances monotonously increase with decreasing temperature because the FISDW gap opens and progressively eliminates free carriers. Below T^* , the R_{xx} can decrease with decreasing temperature since the electron system is in the quantum Hall regime.

The peak temperature T^* shows an unusual field dependence as denoted by dotted curves. The T^* increases until 12 T then decreases with further increasing fields. The highest T^* is ~ 1.5 K at 12 T. Surprisingly, this temperature is in accord with the boundary between two RO's. We found that the RO_B exists below T^* in which the resistance is somewhat metallic, while the RO_A is observable above T^* where the resistance is semiconducting or insulating. We notice that the type of RO, the behavior of the oscillations, temperature, and field dependences of the magnetoresistances between two regions separated by the $T^*(H)$ are completely different. The above fact implies that there would be new subphases whose boundary is $T^*(H)$ in the main FISDW phase above 8 T.

In McKernan's phase diagram, a peculiar FISDW phase boundary is present at 3.5 K from ~ 20 to ~ 25 T and goes down about 27 T, but it does not close up at a lower field than 20 T. Related to the HFS boundary at 3.5 K, we found evidence of the same transition for the lower field side and could complete the boundary of this phase. As shown in Fig. 6(a), the resistance slope at 18 and 20 T changes at ~ 3.3 K, indicating the same HFS transition. On the other hand, we notice a sudden increase of the $R_{zz}(H)$ at ~ 17.5 T below 1.0

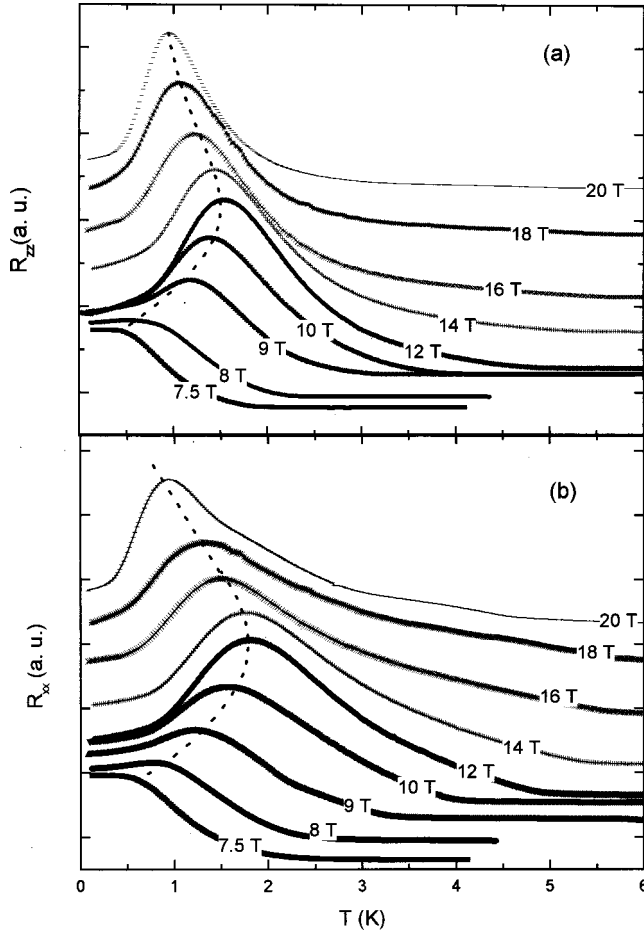


FIG. 5. Temperature dependence of (a) R_{zz} and (b) R_{xx} in various fields. Dotted curve indicates the resistance peak temperature, T^* which depends on the magnetic field. The RO_B is existent below T^* and the RO_A exists above T^* .

K as shown in Fig. 6(b). We draw dotted lines to follow the tendency of the oscillation amplitude and see a clear deviation from the general behavior of the resistance at ~ 17.5 T. We suggest that the sudden changes in the $R_{zz}(H)$ are related to the 3.5 K transition for the lower field side. The possibility of such a transition has been confirmed recently in a study extended to higher fields.^{23,24}

IV. DISCUSSION

A. The origin of two rapid oscillations

Since the RO's in the FISDW phase have different properties in many aspects, the origin of the RO is not as simple as that in the M phase. Although there are several recent explanations for the RO in the FISDW, none of them are satisfactory. Recently, Brooks *et al.*²⁰ suggested that the combination effects of the reconstructed and nested FS, MB, and BR result in closed orbits which causes the conventional SdH or dHvA effects in the HFS above 28 T and below 5.5 K. The temperature and field dependence in this region is explained by the Lifshitz-Kosevich formula with reasonable parameter. Uji *et al.* also ascribed their RO II to dHvA oscillations in the FS reconstructed by the SDW and the AO. McKernan *et al.* suggested that SDW nesting between two FS takes place separately with weak coupling between the

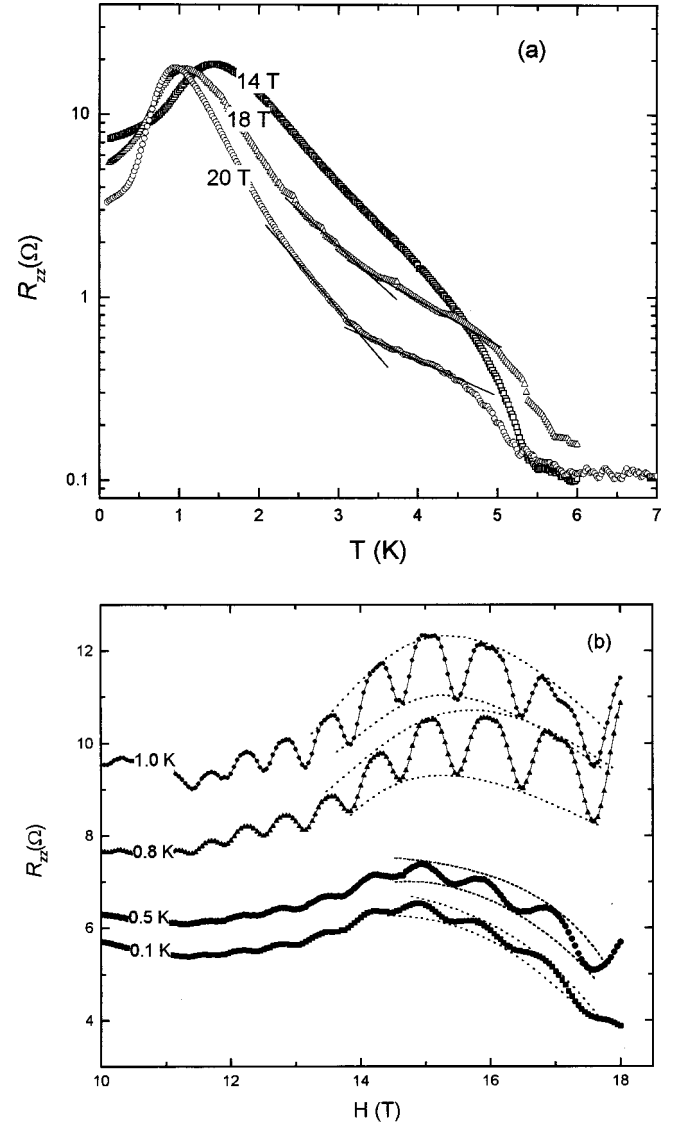


FIG. 6. (a) The R_{zz} exhibits the change of the resistance slope at 18 and 20 T, indicating McKernan's 3.5 K phase boundary. (b) The background R_{zz} increases suddenly at ~ 17.5 T below 1 K. We marked dotted curves for the trace of the oscillation amplitudes.

order parameters, in order to explain their 3.5 K phase boundary above 20 T. However, they conflict with the RO in the FISDW phase below 20 T since these two models explain only the HFS.

The two distinct RO's, the change of the slope in the $R_{xx}(T)$ and in the $R_{zz}(T)$ curves, and different field and temperature dependences between low- and high-temperature regions indicate that there are possibly new subphases whose boundary is the $T^*(H)$ inside of the main FISDW phase. For the origin of the subphases, we consider separate SDW transitions on each pair of Fermi surfaces. As the system is cooled through 5.5 K in fields between 8 and 20 T, the nesting of SDW with wave vector $\mathbf{Q}_A(Q_{Ax} = Q_x + \Delta/\hbar v_F)$ takes place independently in the one pair (FS_A) at 5.5 K and in the other pair (FS_B) with wave vector $\mathbf{Q}_B(Q_{Bx} = Q_x - \Delta/\hbar v_F)$ at T^* as shown in Fig. 1(a).

The M phase with the AO, and the SDW phase coexist between 5.5 K and T^* , corresponding to the situation of Fig. 1(c). Then, the SDW nested FS_A and metallic FS_B coexist

and small electron and hole pockets are formed only on the FS_A [the right FS of Fig. 1(c)], while the other sheet of FS (FS_B) remains metallic. As the MB across the SDW gaps becomes possible upon increasing the field, the electrons on the FS_A proceed either along the same direction, path 1, or along the opposite direction, path 2. Between the FS_B and the reconstructed sheet 1 where the electrons travel along the same direction, the Stark quantum interference takes place even inside the FISDW phase. On the other hand, between the FS_B and the sheet 2 where electrons travel along the opposite direction, the large closed hole orbits are formed by the MB and BR processes. Therefore, the two different mechanisms are involved to generate the oscillations in the resistance. Their periods coincide precisely since the involved orbit areas are the same. The RO_A in the RO_x is the combination of the Stark oscillations and the SdH oscillations, while the oscillations in the RO_z is due to the SdH oscillations since the Stark effect does not exist in the R_{zz} .

As the system is cooled further, the second SDW nesting takes place on the FS_B at the T^* , and electron and hole pockets are also formed on the FS_B [the left FS of Fig. 1(d)]. When the magnetic field is large enough, two large MB orbits (electron and hole orbits) are formed as depicted in Fig. 1(d). This electronic state at low temperatures below T^* is similar to that in the HFS phase. The reconstructed FS gives the possibility of conventional SdH or dHvA effects coming from the MB closed orbits. At T^* (~ 1.5 K), the type of oscillations change from the RO_A to RO_B , which has the same frequency since the orbital area is the same in all three cases. The phase difference by π between two RO 's is not yet understood.

B. The amplitude of the rapid oscillations

The progressive increase of the RO amplitude with increasing field, as observed in Fig. 3, is because the tunneling probability across the SDW gaps increases with increasing field. The MB orbits which are shown in Figs. 1(c) and 1(d) execute cyclic motion and generate SdH oscillations. The SdH oscillation waveform contains higher order. The characteristic field for the MB is assumed to be an increasing function of the SDW gap. Then the oscillation amplitude due to the MB orbits is suppressed by increasing the SDW gap as temperature decrease. Since the SDW gap is involved in the MB orbital motion, the oscillation behavior is expected to be different from that of the conventional SdH oscillations. Under a fixed field, as temperature decreases in the FISDW state, the amplitude of the RO 's are expected to have maxima because of the growth of the SDW gap. This is consistent with the observations (See Fig. 4). The RO eventually vanishes at lower T where the SDW gap ultimately prevents RO . As we mentioned previously, while the crossover between RO_A and RO_B is clearly seen at ~ 1.5 K in the RO_z , the change in the RO_x takes place continuously over wide temperature region about T^* . We believe that the participation of the Stark effect in the RO_x causes the different behavior of the RO 's from the RO_z .

The amplitude of the RO_A is much weaker in the RO_x than in the RO_z , while the RO_B is comparable for both resistances. Possibly, the mixture of the Stark and SdH oscillations in the RO_x weaken the amplitude of the RO_A . But in

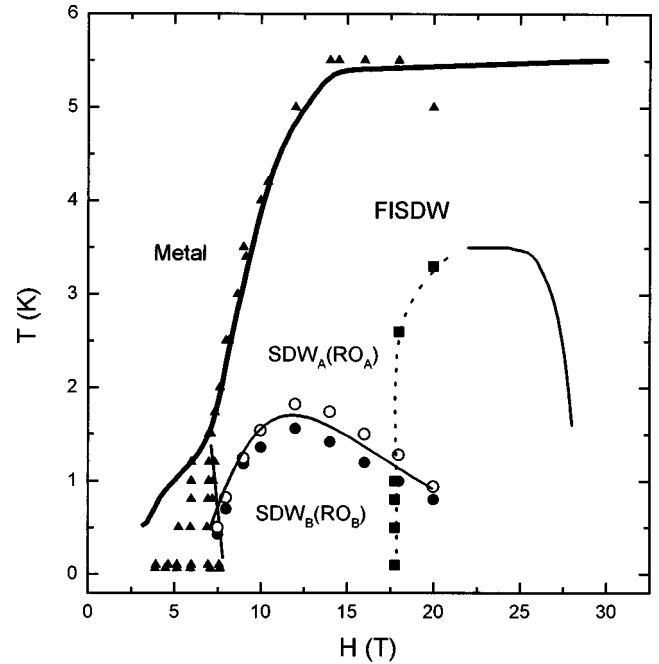


FIG. 7. A new field-temperature phase diagram of $(TMTSF)_2ClO_4$ is established where the $T^*(H)$ (open circles for R_{xx} and solid circles for R_{zz}) is a phase boundary for the RO_A and RO_B . The solid squares indicate where the discontinuous change of the resistance is observed in the R_{zz} and the dotted line is an extension of the low-field boundary of the McKernan's 3.5 K HFS.

the RO_z , only the SdH oscillations by the closed orbit give a strong oscillation. As temperature is lowered below T^* , the Stark oscillations do not exist and the magnitudes of the RO_B in both resistances become comparable. In the RO_z , amplitude of the RO_A is larger than that of RO_B , as shown in Fig. 4(a). This is because the two SDW gaps are involved in the MB orbits in the RO_B , while only one is involved in the RO_A . Therefore, the tunneling probability is reduced in the RO_B state where the oscillation becomes weaker.

C. New subphases in the FISDW phase in $(TMTSF)_2ClO_4$

Figure 7 presents temperature-field phase diagram of this system. Solid triangles indicate transitions of the cascade of the FISDW states in our measurements. The solid lines show the phase boundary proposed by McKernan *et al.* Solid squares in the diagram correspond to the sudden change of the resistance in the $R_{zz}(T)$ or in the $R_{zz}(H)$ [Figs. 6(a) and 6(b)]. The extension of the 3.5 K phase boundary is marked with a dotted line in the phase diagram. Solid and open circles show the $T^*(H)$ in the R_{zz} and in the R_{xx} , respectively. We note that the T^* in the R_{xx} is ~ 0.5 K higher than that in the R_{zz} . Consistently, the crossing from RO_B to RO_A in the RO_x occurs at higher temperatures than in the RO_z . The difference of the crossover temperature can be explained with the temperature dependence of the RO amplitudes. Since the RO_B (RO_A) is stronger than the RO_A (RO_B) in the RO_x (RO_z) as we had mentioned in Fig. 4, stronger oscillations (RO_B for the RO_x) can permeate into the region of weaker oscillation and shift the crossover temperature. Therefore, it is reasonable to draw the boundary between RO_A and RO_B phases.

V. SUMMARY

From a systematic study of longitudinal and transverse magnetoresistances in $(\text{TMTSF})_2\text{ClO}_4$, we found that two distinctly different quantum oscillations exist at different temperature regions in the FISDW phase. The different properties between the RO_A and the RO_B , such as the temperature and field dependences of the RO amplitudes as well as different phase by π and the temperature dependence of the resistance, imply the existence of the subphases in the main FISDW phase. We suggest that the SDW transition takes place separately at 5.5 K and at T^* on each pair of the FS. The amplitude maxima of the RO's at ~ 1 and ~ 3 K are explained by the temperature dependence of the SDW gap.

In addition, we extend the McKernan's 3.5 K phase boundary to the lower side of the field as a result of the sudden increase of the R_{zz} at low temperatures as shown in Fig. 6. Our results conclude that the system has more than two different subphases which are separated by $T^*(H)$ within the FISDW phase of $(\text{TMTSF})_2\text{ClO}_4$.

ACKNOWLEDGMENTS

These experiments were performed by using a 20 T superconducting magnet and dilution refrigerator at Korea Basic Science Institute. This study was supported by the Korea Science and Engineering Foundation under Grant No. 96-0702-04-01-3.

-
- ¹For a review, see T. Ishiguro and K. Yamaji, *Organic Superconductors* (Springer-Verlag, Berlin, 1990).
- ²L. P. Gor'kov and A. G. Lebed', *J. Phys. (France) Lett.* **45**, L-433 (1984); P. M. Chaikin, *Phys. Rev. B* **31**, 4770 (1985); M. Héritier, G. Montambaux, and P. Lederer, *J. Phys. (France) Lett.* **45**, L-943 (1984); K. Yamaji, *J. Phys. Soc. Jpn.* **54**, 1034 (1985); M. Ya Azbel, P. Bak, and P. M. Chaikin, *Phys. Lett. A* **117**, 92 (1986); K. Maki, *Phys. Rev. B* **33**, 4826 (1986).
- ³S. T. McKernan, S. T. Hannahs, U. M. Scheven, G. M. Danner, and P. M. Chaikin, *Phys. Rev. Lett.* **75**, 1630 (1995).
- ⁴M. J. Naughton, R. V. Chamberlin, X. Yan, S. Y. Hsu, L. Y. Chiang, M. Ya Azbel, and P. M. Chaikin, *Phys. Rev. Lett.* **61**, 621 (1988).
- ⁵J. P. Ulmet, L. Bachère, and S. Askenazy, *Solid State Commun.* **58**, 753 (1986).
- ⁶T. Osada, N. Miura, and G. Saito, *Solid State Commun.* **60**, 441 (1986).
- ⁷X. Yan, M. J. Naughton, R. V. Chamberlin, S. Y. Shu, L. Y. Chiang, J. S. Brooks, and P. M. Chaikin, *Phys. Rev. B* **36**, 1799 (1987); X. Yan, M. J. Naughton, R. V. Chamberlin, S. Y. Shu, L. Y. Chiang, and P. M. Chaikin, *Synth. Met.* **27**, B-145 (1987).
- ⁸N. A. Fortune, J. S. Brooks, M. J. Graf, G. Montambaux, L. Y. Chiang, J. A. A. Perenboom, and D. Althof, *Phys. Rev. Lett.* **64**, 2054 (1990).
- ⁹R. C. Yu, L. Y. Chiang, R. Upasani, and P. M. Chaikin, *Phys. Rev. Lett.* **65**, 2458 (1990).
- ¹⁰X. D. Shi, W. Kang, and P. M. Chaikin, *Phys. Rev. B* **50**, 1984 (1994).
- ¹¹C. C. Agosta, D. A. Howe, M. A. Antia, S. A. Ivanov, C. H. Mielke, and F. M. Morgan, in *High Magnetic Fields in the Physics of Semiconductors*, edited by D. Heiman (World Scientific, Singapore, 1995), p. 738.
- ¹²S. Uji, T. Terashima, H. Aoki, J. S. Brooks, M. Tokumoto, S. Takasaki, J. Yamada, H. Anzai, and S. Uji, *Phys. Rev. B* **53**, 14 399 (1996).
- ¹³M. J. Naughton, J. P. Ulmet, I. J. Lee, and J. M. Fabre, *Synth. Met.* **85**, 1531 (1997).
- ¹⁴A. G. Lebed' and P. Bak, *Phys. Rev. B* **40**, 11 433 (1989).
- ¹⁵T. Osada, S. Kagoshima, and N. Miura, *Phys. Rev. Lett.* **69**, 1117 (1992).
- ¹⁶Y. M. Yakovenko, *Phys. Rev. Lett.* **68**, 3607 (1992).
- ¹⁷K. Maki, *Phys. Rev. B* **49**, 12 362 (1994).
- ¹⁸A. G. Lebed', *Phys. Rev. Lett.* **74**, 4903 (1995).
- ¹⁹R. W. Stark and C. B. Friedberg, *J. Low Temp. Phys.* **14**, 111 (1974).
- ²⁰J. S. Brooks, R. G. Clark, R. H. McKenzie, R. Newbury, R. P. Starrett, A. V. Skougarevsky, M. Tokumoto, S. Takahashi, J. Yamada, H. Anzai, and S. Uji, *Phys. Rev. B* **53**, 14 406 (1996).
- ²¹S. Uji, J. S. Brooks, M. Chaparala, S. Takasaki, J. Yamada, and H. Anzai, *Phys. Rev. B* **55**, 14 387 (1997).
- ²²H. Cho and W. Kang, *Phys. Rev. B* **59**, 9814 (1999).
- ²³K. Machida, Y. Hasegawa, M. Kohmoto, V. M. Yakovenko, Y. Hori, and K. Kishigi, *Phys. Rev. B* **50**, 921 (1994).
- ²⁴J. Moser, W. Kang, Haeyong Kang, and D. Jérôme (unpublished).